Direct Observation of Intrinsic Pinning by Layered Structure in Single-Crystal $YBa_2Cu_3O_{7-\delta}$

W. K. Kwok, U. Welp, V. M. Vinokur,[a] S. Fleshler,[b] J. Downey, and G. W. Crabtree
Science and Technology Center for Superconductivity and Materials Science Division, Argonne National Laboratory, Argonne, Illinois 60439
(Received 29 April 1991)

The intrinsic pinning in twinned and untwinned single-crystal $YBa_2Cu_3O_{7-\delta}$ is observed using a novel crossed-magnetic-field technique for obtaining angular resolutions of $\Delta\theta < 0.005°$. The pinning occurs for magnetic-field directions within a critical angle $\theta^* < 1°$ of the Cu-O planes. The data are discussed in the context of a lock-in transition of vortices in the **a-b** plane of the crystal.

PACS numbers: 74.70.Jm, 74.60.Ge

The high-T_c oxide superconductors have layered structures which exhibit strong anisotropy in resistivity [1], the upper critical field H_{c2} [2], and critical current [3]. Large values of critical current and H_{c2} are obtained for the highly conductive Cu-O planes [2,3]. Recently, Tachiki and Takahashi [4] have pointed out an intrinsic pinning mechanism of the vortices when the magnetic field is parallel to the Cu-O planes. They proposed that the modulation of the order parameter perpendicular to the layers can pin the vortices between the layers. Later it was shown that pinning by planar structures occurs only when the misalignment of the field with the plane does not exceed a critical angle θ^* [5,6]. In this Letter we present direct observation of intrinsic pinning by the layered structure in both twinned and untwinned single crystals of $YBa_2Cu_3O_{7-\delta}$, using a novel crossed-magnetic-field technique where angular resolutions of $\Delta\theta < 0.005°$ are obtained. We determine the critical angle for intrinsic pinning and the phase diagram for the onset of intrinsic pinning.

The samples were prepared by a self-flux method described elsewhere [7] which yielded crystal sizes of $1.0\times0.7\times0.04$ mm^3. Untwinned single crystals were obtained by annealing a high-quality single crystal at $\sim$450 °C under uniaxial pressure along one of its **a**,**b** crystallographic axes [8]. Two single crystals were chosen for this experiment, a twinned crystal with twin boundaries in only one of the ⟨110⟩ directions with zero resistance at $T_0 = 90.31$ K and transition width ΔT_c(10%–90%) $\sim$0.14 K, and an untwinned crystal with zero resistance at $T_0 = 90.41$ K and transition width ΔT_c(10%–90%) $\sim$0.34 K.

Resistivity measurements were used as a direct probe of flux-motion dissipation. The resistivity was measured by the standard four-probe ac technique with a typical measuring current density of approximately 0.7 A/cm^2 at 17 Hz applied in the Cu-O plane of the crystal. Gold wires were attached to the sample with silver epoxy, resulting in contact resistances of less than 1 Ω. The sample was placed in the bore of two superconducting magnets, a split coil 1.5-T transverse-mounted magnet which resides within the larger bore of an 8-T longitudinal magnet as shown in the inset of Fig. 1. The sample may be rotated about the axis of the longitudinal magnet, usually corresponding to a crystallographic symmetry axis of the crystal. A qualitative measure of the anisotropy in the flux-flow resistivity can be obtained by rotating the crystal in constant magnetic field and temperature from its low-H_{c2} orientation (**H**‖**c**) to its high-H_{c2} (**H**‖**a-b**) orientation. Figure 1 shows such data for the twinned crystal a 89.88 K and 1.0 T, where θ is the field direction measured from the Cu-O layers in a plane containing the **c** axis. For highly anisotropic superconductors, the flux-motion resistivity is slowly varying and large near $\theta = 90°$, and exhibits a sharp drop near 0°. For the data in Fig. 1, this behavior can be fitted by the empirical form $R(\theta) = R(\mathbf{H}\|\mathbf{c})|\sin\theta|^q$, where $q \sim 0.4$. For more anisotropic materials like oxygen-deficient $YBa_2Cu_3O_{7-\delta}$ and the organic superconductor κ-(BEDT-TTF)$_2$Cu(NCS)$_2$, the value of q decreases [9].

For intrinsic pinning, the region of interest is near $\theta = 0°$ where the magnetic field lies parallel with the Cu-O planes. In order to achieve high angular resolution in this region, we developed a crossed-field technique where the longitudinal magnetic field was held constant and the

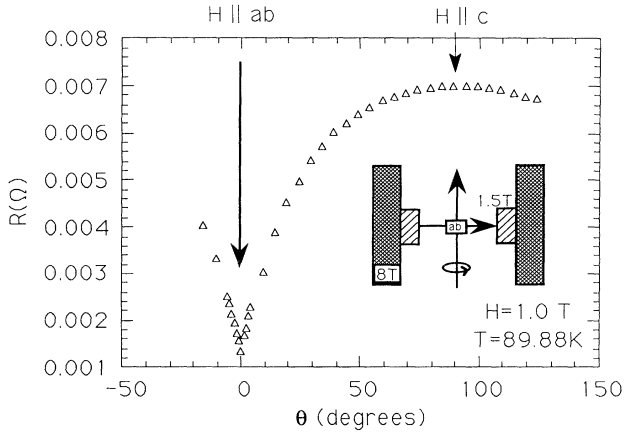

FIG. 1. Angular dependence of the resistance for single-crystal $YBa_2Cu_3O_{7-\delta}$. θ is the magnetic-field angle from the crystallographic **a-b** plane of the crystal. Inset: Schematic of the crossed-field technique.

© 1991 The American Physical Society

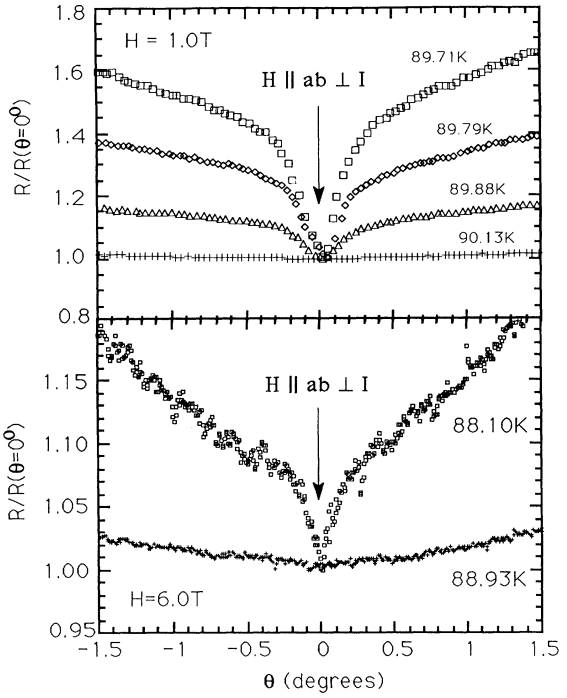

FIG. 2. Angular dependence of the resistance for $H=1.0$ and 6.0 T in the region about the **a-b** plane.

split-coil transverse magnet was swept at a constant rate. Data were collected at constant field intervals. With this method, an angular resolution of $\Delta\theta < 0.005°$ can be obtained.

Figure 2 shows normalized resistivity versus angle near the **a-b** plane for the twinned crystal for several temperatures near T_c in magnetic fields of $H=1.0$ T and 6.0 T. The resistivity was normalized to its value at $\theta=0°$ at each temperature. The sample was mounted such that the measuring current was always perpendicular to the magnetic field. For field directions close to the **a-b** plane, the Lorentz force on the vortices is nearly perpendicular to the Cu-O planes. As the magnetic-field angle with the Cu-O plane approaches zero, a sharp drop in resistivity is observed, signaling the onset of an additional pinning mechanism. The width of the drop is extremely sharp, $\sim 0.6°$ and $\sim 0.5°$ for $H=1.0$ and 6.0 T, respectively. The drop in resistivity $\Delta\rho/\rho$ is about 25% for $H=1.0$ T at 89.71 K and 6% for $H=6.0$ T at 88.1 K and decreases rapidly with increasing temperature. The untwinned crystal showed virtually identical behavior with an angular width of $\sim 0.9°$ for $H=1.0$ T.

To verify that the sharp drop in resistivity for **H||a-b** is due to the inhibition of vortex motion by pinning, we repeated the measurement in a second geometry for which the Lorentz force is approximately zero. The crystal was oriented so that the longitudinal field was parallel to the measuring current in the **a-b** plane. The transverse field

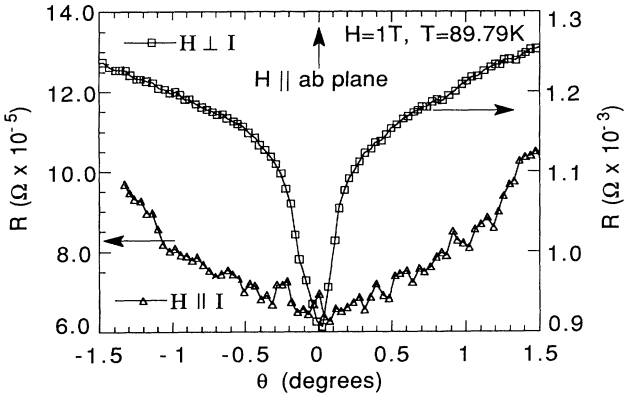

FIG. 3. Comparison of R vs θ for maximum-Lorentz-force ($H \perp I$) and zero-Lorentz-force ($H \| I$) configurations. Both H and I are in the **a-b** plane of the crystal, at $\theta=0$.

from the split-coil magnet was then ramped slowly, tilting the resultant field through the **a-b** plane. For small deviation angles the Lorentz force is small and directed parallel to the Cu-O planes. Data for the $H \| I$ and $H \perp I$ geometries at the same field and temperature are compared in Fig. 3. The total resistivity for $H \| I$ is low because of the reduced flux motion [10]. The smooth dependence of $R(\theta)$ when the field is nearly parallel to the current implies that the sharp drop of $R(\theta)$ for $H \perp I$ is due to the impedance of flux motion perpendicular to the layers, i.e., intrinsic pinning.

Figure 4 shows the phase diagram for the onset of intrinsic pinning and twin-boundary pinning [11] for the twinned crystal obtained from data like that in Fig. 2. At a fixed field aligned with the Cu-O planes or with the twin-boundary planes, $R(\theta)$ was measured for a series of temperatures. The temperature at which the sharp drop in resistivity disappears is taken as the onset temperature. For reference, the zero-resistance temperature and the upper critical field determined from dc SQUID magne-

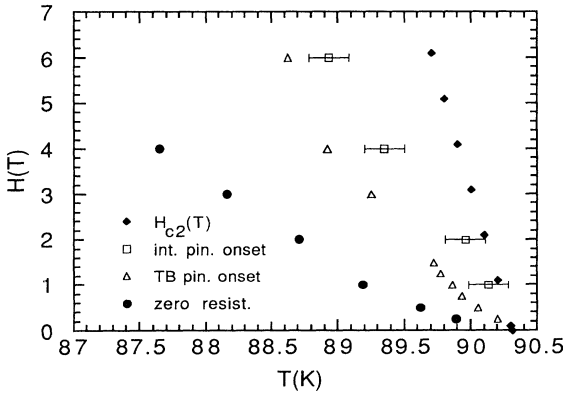

FIG. 4. Phase diagram of the onset of intrinsic and twin-boundary pinning. Estimated upper critical field $H_{c2}(T)$ and measured $H(T_{R=0})$ are shown for comparison.

tometry by Welp *et al.* [2] for the field in the **a-b** plane ($dH_{c2}/dT = -10$ T/K) are also shown. The onset of intrinsic pinning occurs above the onset of twin-boundary pinning. Thus there are two distinct planar pinning mechanisms for vortices in the Cu-O planes: intrinsic pinning by the layered structure which occurs at temperatures very close to T_c, and pinning by twin boundaries which occurs at slightly lower temperatures and is present only for vortices aligned with the twin boundaries.

The original model for intrinsic pinning [4] assumed the vortices to be situated between the layers for magnetic fields in the **a-b** plane. This occurs at low temperatures where the coherence length ξ_c perpendicular to the layers is smaller than the double Cu-O plane spacing, $d = 8$ Å. We observe pinning near T_c where $\xi_c \cong 21$ Å $> d$, so that the vortex core includes more than one period of the washboard potential due to the layered structure. This reduces, but does not eliminate, the effectiveness of the pinning, consistent with the observed minimum in the resistivity for perfect alignment, as opposed to the nearly zero resistivity observed for twin-boundary pinning [10].

It was shown [5,6] that in any periodic pinning potential the flux lines experience a lock-in transition, forcing the vortex lines to lie parallel to the pinning planes at small misalignments of the applied magnetic field. This lock-in transition is identical to the commensurate-incommensurate phase transition in one-dimensional systems [12]. The extremely sharp drop observed in the resistivity may be attributed to this transition for small misalignments of the magnetic field. For larger angles, finite resistivity arises due to creep of vortex lines into adjacent interlayer spaces via the nucleation and motion of kinks along the vortex lines, as shown in Fig. 5. Once a kink has formed, the vortex creeps to the adjacent potential well by a linear motion of the kink parallel to the layers. Above a critical misalignment, multiple-kink creation causes a rapid increase of resistivity with angle. This is analogous to the multiple creation of solitons at a commensurability-incommensurability transition [12].

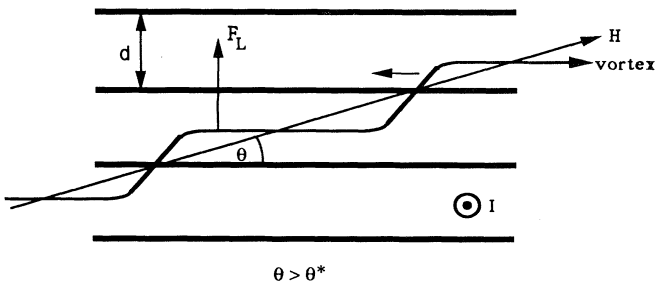

FIG. 5. Schematic diagram of kinks along a vortex line. θ is the magnetic-field angle with respect to the layers and F_L is the Lorentz force acting on vortices parallel to the layers. The small arrow represents the motion of the kinks. Transport current is into the page.

For $YBa_2Cu_3O_{7-\delta}$ the crossover from the quasi-2D ($\xi_c\sqrt{2} < d$) regime to the 3D ($\xi_c\sqrt{2} > d$) behavior takes place at $T \sim 80$ K [13]. Since at the temperature of the experiment ξ_c exceeds d only by a factor of 3, vortices can still "feel" the layered structure of the superconductor. In order to describe the vortex configuration in this case one has to add to the Gibbs potential given by the anisotropic Ginzburg-Landau (GL) theory [14],

$$G(B,\theta) = \frac{B^2}{8\pi} + H^* B\varepsilon(\theta) - \frac{1}{4\pi} BH_i \cos(\theta - \theta_H),$$

the phenomenological periodic potential describing the modulation of the vortex core energy, $[1+\alpha(z)]E_0/a_0^2$. Here $H^* = \Phi_0/(8\pi\lambda_{ab})^2\sqrt{\Gamma}\ln(H_{c2}/B)$, $\varepsilon(\theta) = (\cos^2\theta + \Gamma \times \sin^2\theta)^{1/2}$ is the mass anisotropy function [14], $\Gamma = m_c/m_{ab}$ is the anisotropy parameter, and θ_H and θ are the angles between the **a-b** plane and internal magnetic field H_i and magnetic induction B, respectively. Φ_0 is the flux quantum, $a_0^{-2} = B/\Phi_0$ represents the density of vortex lines,

$$E_0 = \frac{\Phi_0^2}{(4\pi\lambda_{ab})^2\sqrt{\Gamma}} \ln(\kappa\sqrt{\Gamma})$$

is the energy of the single vortex line for $\theta = 0$, when the center of mass of the vortex core lies between the Cu-O planes, $\alpha(z)$ is the positive dimensionless periodic function with amplitude $\alpha < 1$, and κ is the GL parameter. The critical angle θ_i^* between the internal magnetic field and the **a-b** plane can be found by minimizing the total energy with respect to B and θ [5,6]: $\theta_i^* = \eta(2\Delta\varepsilon/\varepsilon_t)^{1/2}$, where $\Delta\varepsilon = \alpha E_0/a_0^2$. ε_t is the tilt modulus which in our case ($H_{c1} \ll B \ll H_{c2}$) is simply $\varepsilon_t = B^2/4\pi$, and η is the numerical factor depending upon the exact form of the washboard pinning potential.

The measured angle θ^* for the lock-in transition is the angle between the external magnetic field H_a and the **a-b** plane, which is related to H_i by $\hat{n}B + (1-\hat{n})H_i = H_a$ [15]. At $\theta < \theta^*$, we have $B_x \cong H_{ix}$ and $B_z = 0$, and one gets $\theta^* = (1-n_{zz})\theta_i^*$ [5,16]. For a crystal of thickness l and width L, $(1-n_{zz}) = \pi l/2L$. Using our values of $H_{c1} \sim 5$ Oe [17], $\kappa = 55$, $H_a = 1$ T, and $\Gamma = 62$ [13], we estimate $\theta^* \sim \sqrt{\alpha}\,\eta$ (0.07°). Since the relative change in resistivity $\Delta\rho/\rho \sim 0.06$–$0.25$ is considerably less than unity, we conclude that even for $\theta = 0$ there is a considerable number of thermally activated kinks which implies the kink energy $E_k \gtrsim T$. Using $E_k = \sqrt{\alpha}\,\eta[\Phi_0^2 d/(4\pi\lambda_{ab})^2]\ln(\kappa\sqrt{\Gamma})$ [5,6] one finds $\sqrt{\alpha}\,\eta \sim 3$. Assuming $\sqrt{\alpha}$ to be close to unity, we obtain $\theta^* \sim 0.21°$ which is close to our measured value of $0.6/2 = 0.3°$. To explain the weak dependence of the critical angle upon magnetic field we note that the resistivity at 88.1 K and 6 T is approximately the same resistivity as for 1 T at 89.71 K. Since we are in the viscous flow region, the resistivity is approximately given by the Bardeen-Stephen formula $\rho = \rho_n H/H_{c2}$ [18] and scales as $\rho \sim H/(T_c - T)$. The critical angle scales as $\theta^* \sim [(T_c - T)/H]^{1/2}$ and consequently should have only

a weak dependence upon magnetic field provided $\rho(H)$ is constant.

Note that below $T=80$ K, the Lawrence-Doniach (LD) model should be employed to describe the vortex structure and the kinks should have the 2D "pancake" structure [19]. In this case, minimization of the free energy (which requires the density of kink energy $BH^*|\theta|$, where $H^*=[\Phi_0/(4\pi\lambda_{ab})^2]\ln(d/\xi_c)$, to be equal to the density of tilt energy $(B^2/8\pi)\theta^2$) gives rise to $\theta^*=(H^*/H)(1-n_{zz})$ [16].

In conclusion, we have observed intrinsic pinning by the layered structure in single-crystal $YBa_2Cu_3O_{7-\delta}$ at surprisingly high temperatures near T_c. We developed a crossed-field technique to obtain angular resolutions of $\Delta\theta<0.005°$, and find the critical angle for intrinsic pinning to be extremely sharp, $\sim 0.5°$ wide. We have obtained the phase diagram for the onset of intrinsic pinning and find it to lie above that of the twin-boundary-pinning phase line. Our results may be explained in terms of a lock-in transition of the vortex lines with respect to the intrinsic pinning potential due to the modulation of the order parameter perpendicular to the Cu-O planes.

The authors would like to thank M. V. Feigelman for helpful discussions. This work was supported by the U.S. Department of Energy, BES-Materials Science under Contract No. W-31-109-ENG-38 (W.K.K., V.M.V., S.F., J.D., G.W.C.), and the NSF Office of Science and Technology Centers under Contract No. STC8809854 (U.W.), Science and Technology Center for Superconductivity.

[a]Also at Institute of Solid State Physics, Chernogolovka, Moscow District, U.S.S.R.

[b]Also at Department of Physics, Purdue University, West Lafayette, IN 47907.

[1] T. K. Worthington, W.J. Gallagher, and T. R. Dinger, Phys. Rev. Lett. **59**, 1160 (1987); Y. Iye, T. Tamegai, H. Takeya, and H. Takei, Technical Report of the Institute for Solid State Physics, University of Tokyo, Ser. A, No. 1919 (1988); J. N. Li, K. Kadowaki, M. J. V. Menken, A. A. Menovsky, and J. J. M. Franse, Physica (Amsterdam) **161C**, 313 (1989).

[2] U. Welp, W. K. Kwok, G. W. Crabtree, K. G. Vandervoort, and J. Z. Liu, Phys. Rev. Lett. **62**, 1908 (1989).

[3] B. Roas, L. Schultz, and G. Saemann-Ischenko, Phys. Rev. Lett. **64**, 479 (1990).

[4] M. Tachiki and S. Takahashi, Solid State Commun. **70**, 291 (1989).

[5] D. Feinberg and C. Villard, Phys. Rev. Lett. **65**, 919 (1990).

[6] G. Blatter, J. Rhyner, and V. M. Vinokur, Phys. Rev. B **43**, 7826 (1991).

[7] D. L. Kaiser, F. Holtzberg, M. F. Chisholm, T. K. Worthington, J. Cryst. Growth **85**, 593 (1987).

[8] U. Welp, M. Grimsditch, H. You, W. K. Kwok, M. M. Fang, G. W. Crabtree, and J. Z. Liu, Physica (Amsterdam) **161C**, 1-5 (1989).

[9] W. K. Kwok (unpublished).

[10] W. K. Kwok, U. Welp, G. W. Crabtree, K. G. Vandervoort, R. Hulscher, and J. Z. Liu, Phys. Rev. Lett. **64**, 966 (1990).

[11] W. K. Kwok, Bull. Am. Phys. Soc. **36**, 336 (1991).

[12] A. L. Fetter and M. J. Stephen, Phys. Rev. **168**, 475 (1968); S. A. Brazovsky, I. E. Dzyaloshinsky, S. P. Obukhov, Zh. Eksp. Teor. Fiz. **72**, 1550 (1977) [Sov. Phys. JETP **45**, 814 (1977)].

[13] D. E. Farrell, J. P. Rice, D. M. Ginsberg, J. Z. Liu, Phys. Rev. Lett. **64**, 1573 (1990).

[14] V. G. Kogan, Phys. Lett. **85A**, 298 (1981); L. J. Campbell, M. M. Doria, and V. G. Kogan, Phys. Rev. B **38**, 2439 (1988).

[15] L. D. Landau and E. M. Lifshitz, *Electrodynamics of the Continuum Media* (Pergamon, Oxford, 1983).

[16] S. S. Maslov and V. L. Pokrovsky, Europhys. Lett. **14**, 591 (1991).

[17] U. Welp *et al.* (to be published).

[18] J. Bardeen and M. J. Stephen, Phys. Rev. A **140**, 1197 (1965).

[19] S. Doniach, in *High Temperature Superconductivity,* edited by K. S. Bedell (Addison-Wesley, Redwood City, CA, 1990), p. 406; J. R. Clem, Phys. Rev. B **43**, 7837 (1991).